MULTIPARAMETRIC QUANTITATIVE MRI ASSESSMENT OF THIGH MUSCLES IN LIMB-GIRDLE MUSCULAR DYSTROPHY 2A AND 2B

FILIPPO ARRIGONI, MD [1] ,[1] ALBERTO DE LUCA, PHD,[2] DANIELE VELARDO, MD,[3] FRANCESCA MAGRI, MD,[4] SANDRA GANDOSSINI, MD,[3] ANNAMARIA RUSSO, MD,[3] MARTIJN FROELING, PHD,[3] ALESSANDRA BERTOLDO, PHD,[5] ALEXANDER LEEMANS, PHD,[2] NEREO BRESOLIN, MD[4] and GRAZIA D'ANGELO, MD, PHD[3]

[1] Neuroimaging Lab, Scientific Institute, IRCCS E. Medea, Via don L. Monza 20, Bosisio Parini, Italy
[2] Image Sciences Institute, University Medical Center Utrecht and University Utrecht, Utrecht, The Netherlands
[3] NeuroMuscular Unit, Scientific Institute, IRCCS E. Medea, Bosisio Parini, Italy
[4] Neurology Unit, IRCCS Foundation Ca' Granda, Ospedale Maggiore Policlinico, Milan, Italy
[5] Department of Information Engineering, Padova University, Padova, Italy

ABSTRACT: *Introduction*: The aim of this study was to apply quantitative MRI (qMRI) to assess structural modifications in thigh muscles of subjects with limb girdle muscular dystrophy (LGMD) 2A and 2B with long disease duration. *Methods*: Eleven LGMD2A, 9 LGMD2B patients and 11 healthy controls underwent a multi-parametric 3T MRI examination of the thigh. The protocol included structural T1-weighted images, DIXON sequences for fat fraction calculation, T2 values quantification and diffusion MRI. Region of interest analysis was performed on 4 different compartments (anterior compartment, posterior compartment, gracilis, sartorius). *Results*: Patients showed high levels of fat infiltration as measured by DIXON sequences. Sartorius and anterior compartment were more infiltrated in LGMD2B than LGMD2A patients. T2 values were mildly reduced in both disorders. Correlations between clinical scores and qMRI were found. *Conclusions*: qMRI measures may help to quantify muscular degeneration, but careful interpretation is needed when fat infiltration is massive.

Muscle Nerve 58:550–558, 2018

In recent years, MRI has been gaining increasing importance in the diagnostic work-up and follow-up of inherited muscular disorders.[1–4] Morphologic imaging based on T1- and T2-weighted conventional sequences has allowed establishment of the pattern and anatomical distribution of muscular degeneration in several muscular disorders including myopathies, Duchenne and Becker muscular dystrophy, and limb girdle muscular dystrophies (LGMD).[1,4–9] Semi-quantitative measures rating the severity of the damage and partially correlating with the clinical performance of patients can be obtained by the visual inspection and evaluation of T1- and T2-weighted images.[10] However, as they are based on the clinical experience and training of the observer, these scales are noncontinuous and nonobjective.[1,4] More advanced approaches, such as fat quantification based on Dixon images, quantitative T2 measurements, diffusion MRI (dMRI), and diffusion tensor imaging (DTI), can obtain observer-independent, quantitative variables and are able to characterize different features of the degenerative processes occurring in the muscular tissue. With Dixon-like sequences it is possible to quantify fat infiltration in muscles, while quantitative T2 values have been related to fat infiltration, edema, inflammation, and changes in fibers structure.[4,11] Finally, DTI derived parameters have proven to be sensitive to muscular modifications occurring after ischemia, exercise, denervation, trauma, and inflammation.[12]

Quantitative MRI (qMRI) techniques (in particular fat quantification with Dixon sequences) have been applied mostly to dystrophinopathies (Duchenne and Becker muscular dystrophy), while very few or no data are available for other, more rare, muscular inherited disorders like LGMDs.[5,11,13–17]

In this study, we applied the above-mentioned qMRI techniques to patients affected by LGMD2A and LGMD2B, which represent the most frequent forms of LGMD in the Italian population.[18] The aims of this work were (i) the quantification of the structural modifications occurring in the thigh muscles, (ii) the identification of (potentially) different patterns of degeneration between the 2 disorders and in different muscular compartments of the thigh, (iii) the identification of MR-derived disease markers correlating with clinical parameters of muscular strength and function.

MATERIALS AND METHODS

Patients. Twenty patients, with a clinical and genetically-confirmed diagnosis of LGMD2A or LGMD2B,[19–22] were included in the study. Eleven healthy age- and sex-matched subjects were recruited as controls (HC).

Clinical evaluations and MRI exams were performed at the Scientific Institute E. Medea by the NeuroMuscular Unit and the Neuroimaging Lab, respectively. This study was approved by the local ethics committee, and informed consent was obtained from all participants.

Clinical and Functional Assessment. Clinically relevant data (age at disease onset, disease duration, and age of loss of walking ability/ambulation) were obtained by a personal interview and from available medical records. Cardiac and respiratory function data were also collected (data not reported). The British Medical Research Council (MRC) scale was used to assess muscle strength.[23] A total of 4 joint movements were tested on both sides (i.e., hip flexion, hip abduction, hip adduction, and knee extension). Motor function measure (MFM) was assessed in all patients by a trained physiotherapist, as previously described[24]; briefly, MFM comprises 32 items, divided into 3 dimensions: standing position and transfers (D1), axial and proximal motor function (D2), distal motor function (D3); a percentage result is attributed to each of the 3 domains and to the overall test (total MFM). Patients still able to walk were also tested by the 6-minute walk test (6MWT).[25–27]

MRI Protocol. All thigh MRI acquisitions were performed with a 3T Philips Achieva dStream scanner (Philips Medical Systems NV, Best, The Netherlands) using a 16-channel body coil coupled with the 12-channel receiver coil embedded in the bed. The acquisition protocol consisted of:

- A fast field echo (FFE) T1-weighted sequence for radiologic purposes, acquired with resolution $1 \times 1 \times 6$ mm^3, 30 slices, echo time, TE = 2 ms, TR = 642 ms, SENSE factor 2, acquisition time 2 min 35 s;
- A Dixon FFE sequence for fat fraction (FF) quantification, acquired with resolution $1 \times 1 \times 6$ mm^3, 40 slices, 12 echoes, flip angle 3°, echo time (TE) = 1.2 ms, inter-echo time 2.7 ms, repetition time (TR) = 16.17 ms, SENSE factor 2, acquisition time 1 min 37 s;
- A multi-echo spin-echo T2 (T2-MESE) sequence with 12 echoes for T2 quantification, acquired with resolution $1.7 \times 1.7 \times 6$ mm^3, 40 slices, TE = 9.3 ms, inter-echo time 12.5 ms, ,TR = 14.3 s, SENSE factor 2, acquisition time 14 min 45 s;
- A multi-shell dMRI sequence including 5 volumes at b = 0 s/mm^2, 16 volumes at b = 250 s/mm^2 and 16 volumes at b = 400 s/mm^2. The data were acquired with resolution $2 \times 2 \times 6$ mm^3, 40 slices, TE = 46 ms, TR = 6 s, SENSE factor 2, acquisition time 11 min 33 s. Fat suppression was performed using SPIR and SPGR approaches.[28,29]

The field of view was centered on the distal part of the weakest thigh, and its positioning standardized from the patella upward. Rectus femoris, vastus medialis, vastus intermedius, vastus lateralis, semitendinosus, semimembranosus, biceps femoris, adductor magnus, and adductor longus were included in the exam. The duration of the MRI exam was approximately 30 minutes.

MRI Data Processing. FF was directly quantified from the scanner software, which uses an IDEAL based algorithm[30,31] to compute water signal (WS) and fat signal (FS) maps while taking into account field inhomogeneity, eddy currents and T2* effect. T$_2$ quantification from the T2-MESE data was performed in MATLAB (Mathworks Inc.) fitting the data to a bi-exponential model to minimize the fat partial volume effect.[32] The model can be written as:

$$S_{T2-MESE} = f_{muscle} e^{-\frac{T_E}{T_{2,.muscle}}} + \left(1 - f_{muscle}\right) e^{-\frac{T_E}{T_{2,fat}}}$$

As previously suggested for T2 quantification in highly fat infiltrated muscles,[33] the fit procedure was implemented in 2 steps. In a first step a mask of the subcutaneous fat was automatically obtained by Otsu thresholding of the last T2 echo,

then the signals within such mask were averaged and fit with a mono-exponential decay to determine $T_{2,fat}$. Once this value was determined, a Non-Linear Least Squares fit of the above equation using the constrained Trust Region Reflective algorithm implemented in MATLAB was performed discarding the first echo, which might be affected by stimulated-echoes artefacts. Estimates were constrained within physiologically plausible values, e.g., $0 \leq$ f_muscle ≤ 1, 10 ms $\leq$ T_(2,-muscle) ≤ 70 ms. The dMRI data of each subject was preprocessed for subject motion and eddy currents with Elastix, realigning each volume to the first nondiffusion weighted with an affine transformation,[34] then the b-matrix was rotated accordingly.[35] Fractional anisotropy (FA) and mean diffusivity (MD) maps were computed with an in-house linear estimator[36] implemented in MATLAB R2015b (MathWorks Inc.). The acquisition of 2 diffusion-weighted shells was performed to improve the robustness of the DTI fit to perfusion biases.[36]

Regions of Interest and Statistical Analysis. Given the high contrast provided by the Dixon WS images, these were chosen as references to manually draw 4 regions of interest (ROIs) for statistical analysis purposes: (1) muscles from the anterior compartment of the thigh (rectus femoris, vastus medialis, vastus intermedius, and vastus lateralis); (2) muscles from the postero-medial compartment of the thigh (semitendinosus, semimembranosus, biceps femoris, adductor magnus, and adductor longus); (3) gracilis muscle; (4) sartorius muscle. Gracilis and sartorius were individually segmented because of the different rate of degenerative changes documented previously.[37–39]

To minimize the inclusion of inter-muscle fasciae in the ROIs, a bidimensional erosion of each ROI slice was performed with a 3×3 structuring element. The dMRI space of each subject was used as reference for the analysis. Fine alignment of the other sequences to the dMRI space was obtained with an optimized registration pipeline based on Elastix. As the 2 images shared the same contrast, the Dixon WS image was nonlinearly registered to the first b = 0 s/mm^2 volume using the normalized cross-correlation metric.[40] In this context, the nonlinear registration was employed to account for the EPI distortions. The 6th echo of the T2-MESE sequence was rigidly registered to the DIXON FS image using the normalized cross-correlation metric, then the computed transformation was concatenated with the DIXON to dMRI transformation to move the quantified T$_2$ maps with 1 interpolation.

Given the high fat infiltration observed in patients, dMRI derived measures were expected to be biased.[16] An approach to minimize this effect is to consider only voxels with FF values below a modest threshold (i.e., 20%), however, this was not feasible in our cohort of highly fat infiltrated patients. For this reason, voxels with FF greater than 70% were not considered in the diffusion analysis. Additionally, we implemented a post hoc correction for FA and MD based on a multi-variate regression model. In particular, the median values of FA, MD, and FF were computed for each ROI and subject, then FA and MD were individually modeled as:

$$FA, MD = \beta_0 + \beta_1 FF + \beta_2 DIAGNOSIS$$

where DIAGNOSIS was a categorical variable equal to 1 for patients and 0 for healthy controls. FA and MD were corrected for fat effect but not for disease effect subtracting only the $\beta_1 FF$ term.

The volume of each ROI was determined and divided by the total acquired to determine the volumetric ROI ratio of each subject, which was compared among groups with double sided *t*-tests. The statistical analysis involved computing the boxplots of the average MRI metrics for each ROI. Differences among muscles and groups were tested with the Wilcoxon rank-sum test and the Ansari-Bradley test for dispersion. Nonparametric tests were used as not all the measures were normally distributed. Correlation of MRI metrics with clinical measures of strength (MRC, total MFM, D1, and D2) and other clinical covariates was evaluated with Pearson correlations.

RESULTS

Clinical and Functional Assessment.

Eleven LGMD2A (M/F: 4/7; mean age, 36.4 ± 9.6 years; range, 22–51 years; median disease duration, 18 years; range, 13–30 years, still ambulant 4/11), 9 LGMD2B (M/F: 5/4; mean age, 49.4 ± 7.3 years; range, 34–57 years; median disease duration 28 years; range, 12–31 years, still ambulant 5/9) and 11 healthy controls (M/F: 6/5; mean age, 44.7 ± 10 years; range, 32–62 years) were included in the study. Table 1 shows demographic data and walking ability of patients. Supplementary Table S1, which is available online, shows the results of muscle strength and motor function assessment in both groups of patients.

MRI Morphologic Changes.

At visual inspection, both T1-weighted images and Dixon WS showed diffuse and severe muscular atrophy, as well as intramuscular fat infiltration and thickening of subcutaneous fat in both groups of patients (Figs. 1 and 2). A specific pattern of degeneration for LGMD2A and LGMD2B subjects could not be identified, although some subtle differences between groups were noted. In LGMD2A (Fig. 1), posterior and medial compartment muscles appeared more severely infiltrated than anterior compartment muscles, whereas in LGMD2B (Fig. 2) anterior and postero-medial muscles appeared equally involved. In both groups, sartorius and gracilis appeared less affected than other muscles. One LGMD2A patient (patient 1) showed a unique pattern: a complete fatty degeneration of semimembranosus, semitendinosus, adductor longus and adductor magnus, and a normal appearance of quadriceps, biceps femoris, sartorius, and gracilis.

MRI Quantitative Changes.

All 4 muscular compartments showed a significant reduction of volume ratio in patients ($P \leq 5 \times 10^{-5}$) compared to healthy controls (except for the sartorius in LGMD2A). No differences in muscular volume were observed between LGMD2A and LGMD2B patients ($P = 0.09$)

Both LGMD2A and LGMD2B patients showed markedly and significantly high levels of fat infiltration in all compartments compared to healthy controls (Fig. 3A; $P \leq 5 \times 10^{-4}$ and $P \leq 5 \times 10^{-3}$, respectively). All muscular compartments in both disorders showed fat substitution of muscular tissue, with values up to 7.5 times higher than normal in posterior muscles of LGMD2B patients. For both groups, fat replacement in posterior muscles was higher than in other muscles. Comparing the 2 dystrophy groups, LGMD2B patients showed higher fat

Table 1. Demographic and clinical data of patients with LGMD2A and LGMD2B

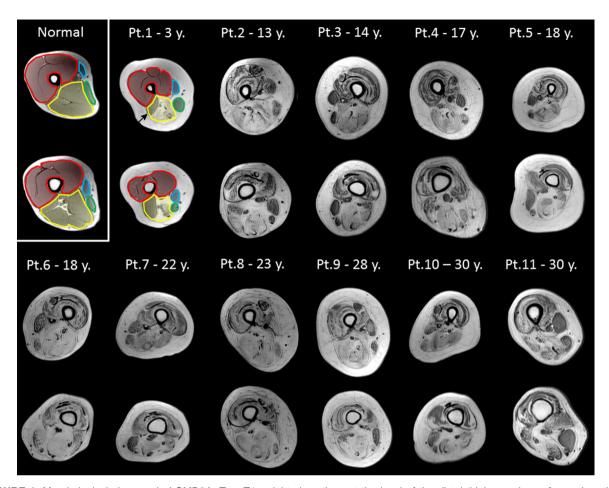| Patient	Diagnosis	Sex	Nucleotide change	Disease duration (years)	Age at onset (years)	Age (years)	Ambulation	Loss of ambulation (years)	6MWT (meters)
1	LGMD 2A	F	c.1193+6 T>A; c.1746-20 C>G	13	30	43	Yes		445.7
2	LGMD 2A	M	c.801+1 G>A; c.550delA	13	17	30	Yes		300
3	LGMD 2A	F	c.550delA	14	8	22	No	20	
4	LGMD 2A	M	c. 883_884 GA>CT + del887A; c.2242 G>A	17	8	25	Yes		few steps
5	LGMD 2A	F	c.328 C>T	18	10	28	No	27	
6	LGMD 2A	M	c.2248 C>T	18	20	38	No	34	
7	LGMD 2A	F	c.1345 A>C	22	16	38	Yes		few steps
8	LGMD 2A	F	c.2330T>C; c.550delA	23	28	51	No	38	
9	LGMD 2A	F	c.550delA; c.1469 G>A	28	13	41	No	28	
10	LGMD 2A	F	c.328 C>T	30	4	34	No	25	
11	LGMD 2A	M	c.1468 C>T, c.2243 G>A	30	20	51	No	45	
	Mean LGMD2A			20.5	15.8	36		31	
12	LGMD2B	F	c.331 C>T	12	22	34	Yes		few steps
13	LGMD2B	M	n.a.	22	20	42	No	40	
14	LGMD2B	F	c.2875 C>T; c.472+2 T>G	25	32	57	Yes		few steps
15	LGMD2B	M	c.2875C>T	26	28	54	Yes		few steps
16	LGMD2B	M	c.2200_2204del	28	21	49	No	41	
17	LGMD2B	M	c.1827T>C; c.2583 T>A; c.2875 C>T	28	27	55	No	43	
18	LGMD2B	F	c.1827T>C; c.2583 T>A; c.2875 C>T	29	23	52	Yes		340.4
19	LGMD2B	F	c.6196 G>A	30	23	53	Yes		few steps
20	LGMD2B	M	c.3113G>A; c.5979InsA	31	18	49	No	42	
	Mean LGMD2B			25.7	23.8	49.4		41.5	

n.a., not available.

FIGURE 1. Morphological changes in LGMD2A. Two T1-weighted sections at the level of the distal thigh are shown for each patient. Disease duration is reported for each subject. Anatomical ROIs used for the analysis are labeled with different colors on a normal subject and on patient 1 as an example (red: anterior compartment, yellow: posterior compartment; light blue: sartorius muscle; green: gracilis muscle). Diffuse, severe fat infiltration is evident for all subjects except for patient 1, who shows a relative sparing of the anterior compartment, gracilis, sartorius, and biceps femoris (arrow). By visual inspection, fat infiltration in the anterior compartment appears to be more severe than in the posterior compartment. [Color figure can be viewed at wileyonlinelibrary.com]

infiltration in the anterior compartment muscles than LGMD2A patients (Fig. 3A).

All compartments in both disorder groups showed significantly reduced T2 values and higher SD than normal subjects (Fig. 3B). In LGMD2A, we found differences in T2 values between posterior muscles and sartorius, while in LGMD2B, differences were detected between anterior and posterior muscles versus gracilis and sartorius. Finally T2 values of the posterior compartment were significantly lower in LGMD2A than LGMD2B (Fig. 3B).

In the intergroup analysis, MD of both patient groups was lower in the anterior compartment compared to HC (Fig. 3C), and characterized by higher dispersion in posterior muscles and gracilis. Physiological differences among intragroup MD values were observed in HC (Fig. 4C), but were not found in the patient groups (except for posterior muscles of LGMD2B patients). Different FA values among compartments were detected in healthy subjects, and partially in LGMD2A, while in LGMD2B the median FA

values of each compartment were not significantly different (Figs. 3 and 4). In LGMD2A patients, posterior muscles had higher FA values than the sartorius and the anterior compartment, whereas the gracilis had higher FA values than anterior muscles (Fig. 3D). When comparing different groups. FA in the posterior compartment were significantly higher in LGMD2A than HC and LGMD2B. Higher FA values were observed also in the anterior muscles for both patient groups compared with HC. Regarding the sartorius muscle, the FA dispersion in HC was significantly lower than both LGMD2A and LGMD2B.

Correlations between MRI Scores and Functional Scales in LGMD2A Patients. FF correlated negatively with Total MFM in both anterior and posterior compartments, and negatively with MRC of quadriceps femoris in the anterior compartment (Fig. 5). No significant correlations emerged between DTI parameters and clinical scores.

Correlations between MRI Scores and Functional Scales in LGMD2B Patients. In LGMD2B patients, neither FF nor T2 values were significantly associated with modifications of total MFM or MRC of adductor and quadriceps. FA and MD of the anterior compartment correlated positively and negatively with MRC of the quadriceps, respectively (Fig. 5).

DISCUSSION

In this multi-parametric MRI study, we assessed morphological and structural modifications of thigh muscles in 2 groups of subjects affected by LGMD2A and 2B muscular dystrophy with long disease duration.

Morphological T1-weighted images revealed severe atrophy of thigh muscles, associated with massive fat infiltrations, as previously reported.[5,39,41,42] Additionally, the use of qMRI showed differences between muscular regions and between HC and patients.

The high levels of fatty infiltration we found are compatible with the long disease duration of our cohort.[43] The LGMD2A patient with normal appearance of quadriceps, biceps femoris, sartorius, and gracilis was among those with the shortest disease duration. This patient also had a peculiar genotype, with 1 missense mutation and 2 intronic variants,

whereas all other LGMD2A patients had 2 missense or at least 1 non-sense/frameshift mutations.

FF and qualitative analysis of T1-weighted images showed a less severe infiltration of the anterior compartment in LGMD2A compared to LGMD2B. Therefore, after a long disease duration, a different pattern of fat deposition can be seen between the 2 disorders.

In healthy subjects, we observed significant differences of DTI parameters (FA and MD) among different compartments (in particular, the anterior and posterior compartments versus sartorius and gracilis). These differences are likely related to variations in muscular structure (e.g., type1/type 2 fiber composition; muscular force; fibers organization within the muscle; type of action: flexion, extension, rotation; fat composition).[44–48] In both LGMD2A and LGMD2B, differences in FA and MD among muscular compartments were less or not significant compared with what was observed in HC. This may be the result of fatty infiltration as well as of fiber degenerative processes that may alter muscular structure, wasting the peculiar organization of each compartment.

T2-values were mildly but significantly reduced in both disorders and in all compartments after
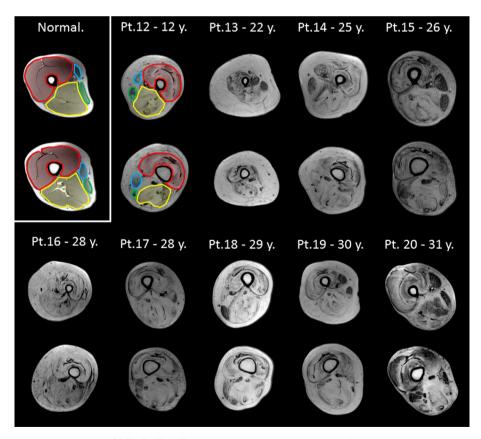

FIGURE 2. Morphological changes in LGMD2B. Two T1-weighted sections at the level of the distal thigh are shown for each patient. Disease duration is reported for each subject. Anatomical ROIs used for the analysis are labeled with different colors on a normal subject and on Patient 1 as an example (red: anterior compartment, yellow: posterior compartment; light blue: sartorius muscle; green: gracilis muscle). The amount of fat replacement and atrophy is marked in all muscular compartments; only the sartorius and gracilis in some patients seem to be relatively spared. [Color figure can be viewed at wileyonlinelibrary.com]
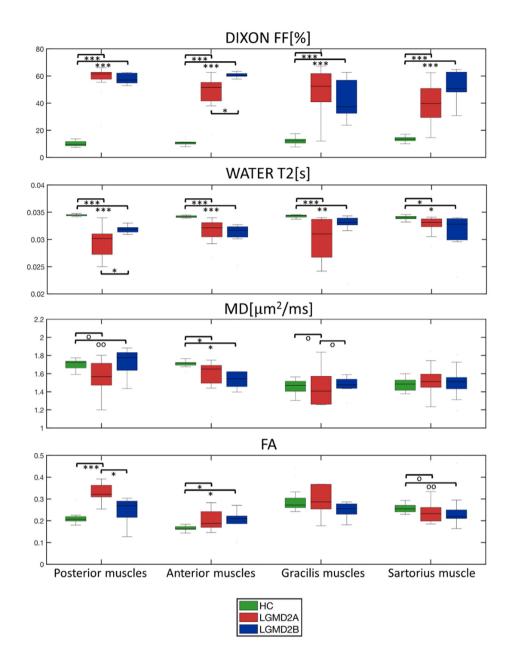
FIGURE 3. Results of quantitative MRI between disorders. The 4 boxplots show the comparison of FF **(A)**, T2 **(B)**, MD **(C)**, and FA **(D)** median values between healthy controls, LGMD2A and LGMD2B. Statistical tests were performed comparing median and dispersion of the groups. Significant differences in median values (Wilcoxon rank-sum test) are reported as follows: *($P \leq 0.05$), **($P \leq 0.005$), ***($P \leq 0.0005$). Significant differences in dispersions (Ansari-Bradley dispersion test) are reported as follows: °($P \leq 0.05$), °°($P \leq 0.005$), °°°($P \leq 0.0005$). [Color figure can be viewed at wileyonlinelibrary.com]

adjusting for fat. The increase in T2-values could be caused by the expansion of interstitial spaces with inflammation.[4] This has been previously reported in several muscular disorders.[49–52] However, in advanced stages of these disorders, significant fibrotic degeneration could cause contraction of water content in the residual tissue and explain the T2-reduction.

The correlations between MRI measures and clinical scores showed that residual strength is related to the amount of fat infiltration in anterior compartments in LGMD2A, including in advanced stages of

the disorder. The same is not valid for our cohort of LGMD2B patients, for which strength was unrelated to fat content.

The correlations between dMRI parameters and MRC scores in LGMD2B patients are more difficult to interpret. A possible explanation is that the architectural/structural integrity or reorganization of the residual muscular fibers may be more important than the fat replacement. Additionally, the deficiency of dysferlin, and its actions of homeostasis and repair of the sarcolemma, in LGMD2B patients could have a
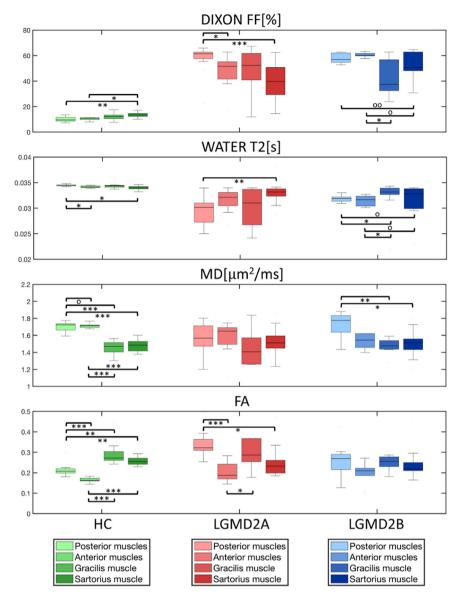
FIGURE 4. Results of quantitative MRI between different regions of interest. The 4 boxplots show the comparison of FF **(A)**, T2 **(B)**, MD **(C)**, and FA **(D)** median values for each muscular compartment, within the same group of subjects (HC, LGMD2A, and LGMD2B). Statistical tests were performed comparing median and dispersion of the groups. Significant differences in median values (Wilcoxon ranksum test) are reported as follows: *($P \leq 0.05$), **($P \leq 0.005$), ***($P \leq 0.0005$). Significant differences in dispersions (Ansari-Bradley dispersion test) are reported as follows: °($P \leq 0.05$), °°($P \leq 0.005$), °°°($P \leq 0.0005$). [Color figure can be viewed at wileyonlinelibrary.com]

direct impact on cell membrane integrity and thus on the diffusion properties of the muscle. A histological confirmation of these specific findings in LGMD2B patients could support such hypothesis.

Our study has some limitations. The number of patients recruited is relatively small and the amount of fat infiltration of the thigh was very high, with reduced residual muscular tissue. Also, our ROIs may have included part of muscular fasciae between different muscles. These factors prevent us from generalizing our conclusions to the overall populations of LGMD2A and LGMD2B patients, in particular with those with shorter disease durations.

The acquisition protocol, and in particular the T2 quantification was overall lengthy, and might be challenging to perform in some clinical settings. However, in this study we used an extensive feet–head coverage of approximately 240 mm, which can be substantially reduced in applications. Furthermore, the acquisition time could be reduced by up to a factor of 3 by taking into account approaches such as multi-band for EPI diffusion imaging,[53] or k-space undersampling and compress sensing for T2 quantification.[54,55] Although the measures we calculated had the advantage of being nonobserver dependent and based on quantitative data derived from the
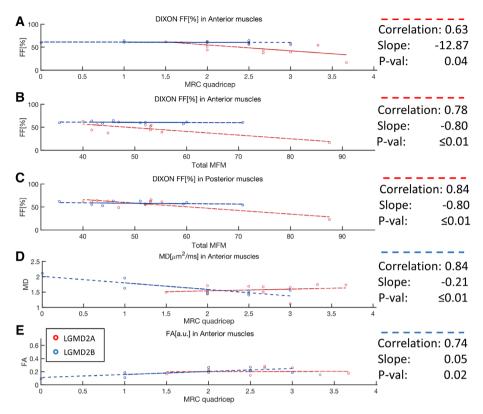
FIGURE 5. Correlations between FF in anterior muscles and MRC quadriceps **(A)** and total MFM **(B)**, FF in posterior muscles and total MFM **(C)**, MRC quadriceps and MD **(D)**, FA and MRC quadriceps **(E)**. ρ and P are the Pearson correlation coefficient and significance, respectively, whereas slope refers to the slope of a linear regression. Only significant correlations between qMRI measures and clinical indexes are reported. [Color figure can be viewed at wileyonlinelibrary.com]

MRI, it must be emphasized that extensive processing is needed to obtain reliable data. Despite the high-resolution MR protocol, the accurate methodology of analysis and the correction applied to reduce the effect of fat replacement on quantitative measurements (T2 and dMRI), it is still possible that these measures were partially affected by fat contamination.

According to our results, FF and volumetric changes of muscular compartments represent reliable quantitative measures to differentiate disorders and quantify muscular degeneration even many years after symptom onset. T2 quantification and dMRI seem to be helpful in characterizing the structural modifications occurring in the tissue, showing some correlations with clinical scores. However, given the possible confounding effects due to the high fat infiltration, we do not recommend them as an independent biomarker in patients with highly atrophic muscular tissue and massive fat infiltration. T2 values and dMRI are probably more informative in subjects with more preserved muscles.

In summary, in patients with advanced stages of LGMD2A and 2B, we quantified the amount of fat infiltration in thigh muscles, described partially different patterns of degeneration between the 2 disorders and among muscular compartments, and identified correlations between qMRI measures and clinical scores.

REFERENCES

1. Leung DG. Magnetic resonance imaging patterns of muscle involvement in genetic muscle diseases: a systematic review. J Neurol 2017;264:1320–1333.
2. Mercuri E, Pichiecchio A, Allsop J, Messina S, Pane M, Muntoni F. Muscle MRI in inherited neuromuscular disorders: past, present, and future. J Magn Reson Imaging 2007;25:433–440.
3. Wattjes MP, Kley RA, Fischer D. Neuromuscular imaging in inherited muscle diseases. Eur Radiol 2010;20:2447–2460.
4. Damon BM, Li K, Bryatn ND. In: Aminoff MJ, Boller F, Swaab DF, editors. *Handbook of clinical neurology*. New York: Elsevier; 2016.
5. Straub V, Carlier PG, Mercuri E. TREAT-NMD workshop: pattern recognition in genetic muscle diseases using muscle MRI: 25-26 February 2011, Rome, Italy. 2012;22:42–53.
6. Faridian-Aragh N, Wagner KR, Leung DG, Carrino JA. Magnetic resonance imaging phenotyping of Becker muscular dystrophy. Muscle Nerve 2014;50:962–967.
7. Filli L, Winklhofer S, Andreisek G, Del Grande F. Imaging of myopathies. Radiol Clin North Am 2017;55:1055–1070.
8. Ten Dam L, van der Kooi AJ, Verhamme C, Wattjes MP, de Visser M. Muscle imaging in inherited and acquired muscle diseases. Eur J Neurol 2016;23:688–703.
9. Kinali M, Arechavala-Gomeza V, Cirak S, Glover A, Guglieri M, Feng L, et al. Muscle histology vs MRI in Duchenne muscular dystrophy. Neurology 2011;76:46–353.

10. Mercuri E, Talim B, Moghadaszadeh B, Petit N, Brockington M, Counsell S, et al. Clinical and imaging findings in six cases of congenital muscular dystrophy with rigid spine syndrome linked to chromosome 1p (RSMD1). Neuromuscul Disord 2002;12:631–638.

11. Burakiewicz J, Sinclair CDJ2, Fischer D, Walter GA, Kan HE, Hollingsworth KG. Quantifying fat replacement of muscle by quantitative MRI in muscular dystrophy. J Neurol 2017;264:2053–2067.

12. Oudeman J, Nederveen AJ, Strijkers GJ, Maas M, Luijten PR, Froeling M. Techniques and applications of skeletal muscle diffusion tensor imaging: a review. 2016;43:773–788.

13. Mankodi A, Azzabou N, Bulea T, Reyngoudt H, Shimellis H, Ren Y, Kim E, et al. Skeletal muscle water T2 as a biomarker of disease status and exercise effects in patients with Duchenne muscular dystrophy. Neuromuscul Disord 2017;27:705–714.

14. Ricotti V, Evans MR, Sinclair CD, Butler JW, Ridout DA, Hogrel JY, et al. Upper limb evaluation in Duchenne Muscular Dystrophy: fat-water quantification by MRI, muscle force and function define endpoints for clinical trials. PLoS One 2016;11:e0162542.

15. Li GD, Liang YY, Xu P, Ling J, Chen YM. Diffusion-tensor imaging of thigh muscles in Duchenne Muscular Dystrophy: correlation of apparent diffusion coefficient and fractional anisotropy values with fatty infiltration. AJR Am J Roentgenol 2016;206:867–870.

16. Hooijmans MT, Damon BM, Froeling M, Versluis MJ, Burakiewicz J, Verschuuren JJ, et al. Evaluation of skeletal muscle DTI in patients with duchenne muscular dystrophy. NMR Biomed 2015;28:1589–1597.

17. Willis TA, Hollingsworth KG, Coombs A, Sveen ML, Andersen S, Stojkovic T, et al. Quantitative magnetic resonance imaging in limb-girdle muscular dystrophy 2I: a multinational cross-sectional study. PLoS One 2014;9:e090377.

18. Magri F, Nigro V, Angelini C, Mongini T, Mora M, Moroni I, et al. The italian limb girdle muscular dystrophy registry: relative frequency, clinical features, and differential diagnosis. Muscle Nerve 2017;55:55–68.

19. Bushby K. Diagnosis and management of the limb girdle muscular dystrophies. Pract Neurol 2009;9:314–323.

20. Guglieri M, Straub V, Bushby K, Lochmuller H. Limb-girdle muscular dystrophies. Curr Opin Neurol 2008;21:576–584.

21. Nigro V, Aurino S, Piluso G. Limb girdle muscular dystrophies: update on genetic diagnosis and therapeutic approaches. Curr Opin Neurol 2011;24:429–436.

22. Thompson R, Straub V. Limb-girdle muscular dystrophies — international collaborations for translational research. Nat Rev Neurol 2016; 12:294–309.

23. Medical Research Council of the UK. Aids to the examination of the peripheral nervous system, memorandum no. 45. Kent, UK: Bailliere Tindall; 1986.

24. Berard C, Payan C, Hodgkinson I, Fermanian J. A motor function measure for neuromuscular diseases. Construction and validation study. Neuromuscul Disord 2005;15:463–470.

25. McDonald CM, Henricson EK, Han JJ, Abresch RT, Nicorici A, Elfring GL, et al. The 6-minute walk test as a new outcome measure in Duchenne muscular dystrophy. Muscle Nerve 2010;41:500–510.

26. ATS statement: guidelines for the six-minute walk test. Am J Respir Crit Care Med 2002;166:111–117.

27. Florence JM, A. van der Ploeg A, Clemens PR, Escolar DM, P. Laforet P, Rosenbloom B, et al. T.P.1.01 Use of the 6 min walk test as an endpoint in clinical trials for neuromuscular diseases. Neuromuscul Disord 2017;18:738–739.

28. Park HW, Kim DJ, Cho ZH. Gradient reversal technique and its applications to chemical-shift-related NMR imaging. Magn Reson Med 1987;4: 526–536.

29. Nagy Z, Weiskopf N. Efficient fat suppression by slice-selection gradient reversal in twice-refocused diffusion encoding. Magn Reson Med 2008; 60:1256–1260.

30. Reeder SB, Pineda AR, Wen Z, Shimakawa A, Yu H, Brittain JH, et al. Iterative decomposition of water and fat with echo asymmetry and least-squares estimation (IDEAL): application with fast spin-echo imaging. Magn Reson Med 2005;54:636–644.

31. Yu H, Shimakawa A, McKenzie CA, Brodsky E, Brittain JH, Reeder SB. Multiecho water-fat separation and simultaneous R2* estimation with multifrequency fat spectrum modeling. Magn Reson Med 2008;60: 1122–1134.

32. Yao L, Yip AL2, Shrader JA3, Mesdaghinia S2, Volochayev R2, Jansen AV, et al. Magnetic resonance measurement of muscle T2, fat-corrected T2 and fat fraction in the assessment of idiopathic inflammatory myopathies. Rheumatology (Oxford) 2016;55:441–449.

33. Azzabou N, Loureiro de Sousa P, Caldas E, Carlier PG. Validation of a generic approach to muscle water T2 determination at 3T in fat-infiltrated skeletal muscle. J Magn Reson Imaging 2015;41:645–653.

34. Klein S, Staring M, Murphy K, Viergever MA, Pluim JPW. elastix: a toolbox for intensity-based medical image registration. IEEE Trans Med Imaging 2010;29:196–205.

35. Leemans A, Jones DK. The B-matrix must be rotated when correcting for subject motion in DTI data. Magn Reson Med 2009;61:1336–1349.

36. De Luca A, Bertoldo A, Froeling M. Effects of perfusion on DTI and DKI estimates in the skeletal muscle. Magn Reson Med 2017;78: 233–246.

37. Paradas C, Llauger J, Diaz-Manera J, Rojas-García R, De Luna N, Iturriaga C, et al. Redefining dysferlinopathy phenotypes based on clinical findings and muscle imaging studies. Neurology 2010;75: 316–323.

38. Kesper K, Kornblum C, Reimann J, Lutterbey G. Pattern of skeletal muscle involvement in primary dysferlinopathies: a whole-body 3.0-T magnetic resonance imaging study. Acta Neurol Scand 2009;120: 111–118.

39. Mercuri E. et al. Muscle MRI findings in patients with limb girdle muscular dystrophy with calpain 3 deficiency (LGMD2A) and early contractures. Neuromuscul Disord 2005;15:164–171.

40. Avants BB, Epstein CL, Grossman M, Gee JC. Symmetric diffeomorphic image registration with cross-correlation: evaluating automated labeling of elderly and neurodegenerative brain. Med Image Anal 2008;12: 26–41.

41. Jin S, Du J, Wang Z, Zhang W, Lv H, Meng L, et al. Heterogeneous characteristics of MRI changes of thigh muscles in patients with dysferlinopathy. Muscle Nerve 2016;54:1072–1079.

42. Diaz J, Woudt L, Suazo L, Garrido C, Caviedes P, CÁrdenas AM, et al. Broadening the imaging phenotype of dysferlinopathy at different disease stages. Muscle Nerve 2016;54:203–210.

43. Fanin M, Nardetto L, Nascimbeni AC, Tasca E, Spinazzi M, Padoan R, et al. Correlations between clinical severity, genotype and muscle pathology in limb girdle muscular dystrophy type 2A. J Med Genet 2007;44:609–614.

44. Scheel M, Prokscha T, von Roth P, Winkler T, Dietrich R, Bierbaum S, et al. Diffusion tensor imaging of skeletal muscle–correlation of fractional anisotropy to muscle power. Rofo 2013;185:857–861.

45. Scheel M, von Roth P, Winkler T, Arampatzis A, Prokscha T, Hamm B, et al. Fiber type characterization in skeletal muscle by diffusion tensor imaging. NMR Biomed 2013;26:1220–1224.

46. Galban CJ, Maderwald S, Uffmann K, de Greiff A, Ladd ME. Diffusive sensitivity to muscle architecture: a magnetic resonance diffusion tensor imaging study of the human calf. Eur J Appl Physiol 2004;93:253–262.

47. Sinha S, Sinha U. Reproducibility analysis of diffusion tensor indices and fiber architecture of human calf muscles in vivo at 1.5 Tesla in neutral and plantarflexed ankle positions at rest. J Magn Reson Imaging 2011;34:107–119.

48. Damon BM, Heemskerk AM, Ding Z. Polynomial fitting of DT-MRI fiber tracts allows accurate estimation of muscle architectural parameters. Magn Reson Imaging 2012;30:589–600.

49. Huang Y, , Majumdar S, Genant HK, Chan WP, Sharma KR, Yu P, et al. Quantitative MR relaxometry study of muscle composition and function in Duchenne muscular dystrophy. J Magn Reson Imaging 1994;4:59–64.

50. Kim HK, Laor T, Horn PS, Racadio JM, Wong B, Dardzinski BJ. T2 mapping in Duchenne muscular dystrophy: distribution of disease activity and correlation with clinical assessments. Radiology 2010;255: 899–908.

51. Hiba B, Richard N, Hébert LJ, Coté C, Nejjari M, Vial C, et al. Quantitative assessment of skeletal muscle degeneration in patients with myotonic dystrophy type 1 using MRI. J Magn Reson Imaging 2012;35:678–685.

52. Willcocks RJ, , Arpan IA, Forbes SC, Lott DJ2, Senesac CR, Senesac E, Deol J, et al. Longitudinal measurements of MRI-T2 in boys with Duchenne muscular dystrophy: effects of age and disease progression. Neuromuscul Disord 2014;24:393–401.

53. Barth M, Breuer F, Koopmans PJ, Norris DG, Poser BA. Simultaneous multislice (SMS) imaging techniques. Magn Reson Med 2016;75:63–81.

54. Sénégas J, Liu W, Dahnke H, Song H, Jordan EK, Frank JA. Fast T(2) relaxometry with an accelerated multi-echo spin-echo sequence. NMR Biomed 2010;23:958–967.

55. Bai R, Cloninger A, Czaja W, Basser PJ. Efficient 2D MRI relaxometry using compressed sensing. J Magn Reson 2015;255:88–99.